Band Structure Calculations of Si-Ge-Sn Alloys: Achieving direct band gap materials

Pairot Moontragoon, Zoran Ikonić, and Paul Harrison

Institute of Microwave and Photonics, School of Electronic and Electrical Engineering, University of Leeds, Leeds, LS2 9JT, United Kingdom

E-mail: eenpm@leeds.ac.uk

Abstract. Alloys of silicon (Si), germanium (Ge) and tin (Sn) are continuously attracting research attention as possible direct band gap semiconductors with prospective applications in optoelectronics. The direct gap property may be brought about by the alloy composition alone or combined with the influence of strain, when an alloy layer is grown on a virtual substrate of different composition. In search for direct gap materials, the electronic structure of relaxed or strained $Ge_{1-x}Sn_x$ and $Si_{1-x}Sn_x$ alloys, and of strained Ge grown on relaxed $Ge_{1-x-y}Si_xSn_y$, was calculated by the self-consistent pseudo-potential plane wave method, within the mixed-atom supercell model of alloys, which was found to offer a much better accuracy than the virtual crystal approximation. Expressions are given for the direct and indirect band gaps in relaxed $Ge_{1-x}Sn_x$, strained Ge grown on relaxed $Si_xGe_{1-x-y}Sn_y$, and for strained $Ge_{1-x}Sn_x$ grown on a relaxed $Ge_{1-y}Sn_y$ substrate, and these constitute the criteria for achieving a (finite) direct band gap semiconductor. Roughly speaking, good-size (up to ∼0.5 eV) direct gap materials are achievable by subjecting Ge or $Ge_{1-x}Sn_x$ alloy layers to an intermediately large tensile strain, but not excessive because this would result in a small or zero direct gap (detailed criteria are given in the text). Unstrained $Ge_{1-x}Sn_x$ bulk becomes a direct gap material for Sn content of $> 17\%$, but offers only smaller values of the direct gap, typically $\leq$0.2 eV. On the other hand, relaxed Sn_xSi_{1-x} alloys do not show a finite direct band gap.

PACS numbers: 71.20.Mq, 71.15.-m, 71.22.+i

1. Introduction

Recent years have witnessed a widespread use of optoelectronic devices. This technology relies on direct band gap III-V materials like GaAs, which is expensive and highly toxic. An interesting alternative would be a direct gap alloy based on group IV materials Si, Ge, and Sn, which are generally compatible with silicon technology, and this has been widely investigated. However, early studies of epitaxial SiGeSn alloys have revealed the difficulties of their growth, with the exception of $Si_{1-x}Ge_x$ binary alloys. With large lattice mismatch between α-Sn (6.489 Å) and Ge (5.646 Å) or Si (5.431 Å), approximately 15% and 17% respectively, and the instability of cubic α-Sn above 13^o C, bulk alloys with Sn cannot be readily grown [1]. Furthermore, because of a lower surface free energy of alpha-tin and germanium, there can be segregation on the surface [2]. These difficulties have been overcome by low temperature molecular beam epitaxy (MBE), which has enabled epitaxial growth of e.g. strained $Ge_{1-x}Sn_x$ superlattices [3] and random $Ge_{1-x}Sn_x$ alloys [4] on a Ge substrate. However, these are not expected to show an indirect-direct transition [1], because of their compressive strain: it is presently believed that a direct gap can only appear in tensilely strained or relaxed $Ge_{1-x}Sn_x$, e.g. [5]. Further advances were made by ultra-high-vacuum chemical vapor deposition (UHV-CVD) and uniform homogeneous relaxed $Ge_{1-x}Sn_x$ alloys with $x < 0.2$ have been grown on silicon[6, 7]. Experimental investigations revealed significant changes in optical constants and redshifts in the interband transition energy as x varied [8], indicating wide tunability of the band gap of these alloys.

The binary GeSn and ternary SiGeSn alloys are considered to be very prospective materials for infrared detectors, as pointed at by Soref and Perry [9], who used linear interpolation scheme to calculate the electronic band structure and optical properties of $Ge_{1-x-y}Si_xSn_y$ alloys and concluded that these will be tunable direct band gap semiconductors. Furthermore, both the direct and indirect band gap in Ge decrease with tensile strain, but the former (initially 140 meV above) does so faster, eventually delivering a direct gap material. Therefore, one can use strained Ge, grown on ternary $Ge_{1-x-y}Si_xSn_y$ alloys [10, 11]. There have since been a number of theoretical investigations of the electronic structure of SiGeSn alloys and the influence of composition fluctuations. For instance, using the tight-binding method within the virtual crystal approximation (VCA), the bowing parameter b_{GeSn} value of 0.30 eV [12] for $Ge_{1-x}Sn_x$ was calculated, while another, pseudopotential based calculation [13] gave the value of -0.40 eV. The latter also predicted that $Ge_{1-x}Sn_x$ alloys become direct gap materials, with $0.55 > E_g > 0$ eV for $0.2 < x < 0.6$. The results for b_{GeSn} are quite remote from each other (even in sign), and both grossly deviate from the experimental value, b_{GeSn}= 2.8 eV [1, 5]. This clearly indicates that VCA cannot explain the behaviour of disordered $Ge_{1-x}Sn_x$ alloys [14], although it is considered reasonably accurate for $Si_{1-x}Ge_x$. In order to take into account the alloy disorder effects, the Coherent Potential Approximation (CPA) was employed for $Si_{1-x}Ge_x$ alloys. According to Chibane *et al.* [15], who used the model developed by Zunger *et al.* [16], the

calculated optical band gap gap bowing is in good agreement with experiment for small Sn contents. However, so far there is no theoretical model which properly describes the optical properties of GeSiSn alloys in a wide range of compositions. The aim of this work is to theoretically explore various possibilities of achieving tunable direct gap semiconductors based on group IV materials, and to investigate the composition dependence of their electronic and optical properties.

2. Computational method

For band structure calculation of SiGeSn alloys we use the charge self-consistent pseudopotential $X\alpha$ method. It finds the self-consistent solution of the Schrödinger equation, with the lattice constituents described by ionic pseudopotential formfunctions. Compared to the first-principles density functional theory in the local density approximation [17, 18], which perform the total energy minimization, the $X\alpha$ method is able to reproduce the electronic structure (i.e. the band gaps, or optical properties of semiconductors) with very good accuracy, without any additional schemes like GW approximation or "scissors correction" as are employed in total energy approaches. On the other hand, this method would not deliver the ground state properties (e.g. the atomic coordinates relaxation, or lattice constant bowing) very accurately, though these can be externally supplied to the calculation. Since our interest in this work are the electronic properties, the $X\alpha$ method was adopted, and experimentally obtained lattice parameters were used where avilable. The calculation starts with the construction of the effective potential, including the pseudopotential, the Hartree potential and the exchange-correlation potential

$$V_{eff}(\mathbf{r}) = V_{ps} + V_{Hartree}(\mathbf{r}) + V_{xc}(\mathbf{r}), \tag{1}$$

where $V_{Hartree}(\mathbf{r}) = \int \frac{e^2 n(\acute{\mathbf{r}})}{|\mathbf{r}-\acute{\mathbf{r}}|} d\acute{\mathbf{r}}$, and $n(\mathbf{r})$ is the real-space electron density. The Hartree potential is evaluated in momentum space

$$V_{Hartree}(\mathbf{q}) = 4\pi e^2 \frac{n(\mathbf{q})}{q^2}, \tag{2}$$

where $\mathbf{q}$ is the wave vector and $n(\mathbf{q})$ are the Fourier coefficients of charge density. This is evaluated in two steps. First, the density was computed on a $16 \times 16 \times 16$ grid of the simple unit cell in real space. Second, the fast Fourier transform was used to transform from $n(\mathbf{r})$ to $n(\mathbf{q})$. The exchange-correlation potential was evaluated in a similar manner. The local exchange-correlation potential of the Slater type has been chosen, defined as

$$V_{xc}(\mathbf{q}) = -\alpha \frac{3}{2} e^2 \left(\frac{3}{\pi}\right)^{\frac{1}{3}} [n(\mathbf{q})]^{\frac{1}{3}}, \tag{3}$$

where $[n(\mathbf{q})]^{\frac{1}{3}}$ are the Fourier coefficients of the cube root of charge density. Based on the approximation of Slater [19], α is a constant which Schlüter *et al.* [20] have set to 0.79. The calculation of this potential was similar to the calculation of $n(\mathbf{q})$, except

that the cube root of $n(\mathbf{r})$ on the cubic grid was taken before transforming from $[n(\mathbf{r})]^{\frac{1}{3}}$ to $[n(\mathbf{q})]^{\frac{1}{3}}$ by fast Fourier transform. The $V_{xc}(\mathbf{q})$ was then evaluated using Eq. (3). As for the pseudopotential, we have used the same form as Srivastava [21],

$$V_{ps}(q) = \left(\frac{b_1}{q^2}\right)(\cos(b_2 q) + b_3)\exp(-b_4 q^4), \tag{4}$$

with the parameters for Si, Ge, and Sn given in Table 1. These are slightly readjusted values from those given in Ref. [21], as dictated by a larger energy cutoff, and a different method of integration over the Brillouin zone, used in this work.

Parameter	Si	Ge	Sn
b_1(Ry)	-1.213	-1.032	0.401
b_2	0.785	0.758	1.101
b_3	-0.335	-0.345	0.041
b_4	0.020	0.024	0.018

Table 1. Parameters of the pseudopotential of Si, Ge and α-Sn

The electronic structure is found by solving the Kohn-Sham equation (in atomic units $\hbar = 2m_e = \frac{e^2}{2} = 1$):

$$\left[-\nabla^2 + V_{eff}(\mathbf{r})\right]\psi_n(\mathbf{k};\mathbf{r}) = \epsilon_n(\mathbf{k};\mathbf{r})\,\psi_n(\mathbf{k};\mathbf{r}), \tag{5}$$

which is done using the self-consistent pseudopotential plane waves method [22], with a kinetic energy cutoff of 24 Ry, the value which gives good convergence of the calculation. The improved linear tetrahedral method [23] was used for integration over the Brillouin zone, with 34 k-points in the irreducible wedge. The convergence of the self-consistent calculation was considered to be adequate when the total energy of the system was stable to within 10^{-3} Ry. In these calculations we do not account for the spin-orbit coupling, because it would double the size of the problem while not being essential for the aim of this work, which is to find whether the smallest band gap is direct or indirect (and this is determined only by the behaviour of the conduction band). Including the spin-orbit coupling would bring slight quantitative corrections in the calculated values of band gaps (with the ionic pseudopotential formfunctions re-adjusted to reproduce the known experimental values for elemental Si, Ge and Sn in this case), but this would not affect the predicted direct-indirect crossover points. Similar conclusion on a relatively small influence of spin-orbit coupling on the topic of interest here has been drawn in [24], based on empirical pseudopotential calculations in the Ge-Sn alloy.

The calculated band structure of bulk Si, Ge, and α-Sn are given in Fig. 1, with the band gap of Si (Ge) being 1.2 eV (0.71 eV), while α-Sn has zero direct band gap. The longitudinal (m_l) and transverse effective mass (m_t) for the X-valley in Si are $0.87m_0$ and $0.22m_0$. Similarly, the L-valley in Ge has m_l =$1.68m_0$ and m_t =$0.16m_0$. All these are in very good agreement with the published values, indicating that the parameters can be reliably used for further calculations.

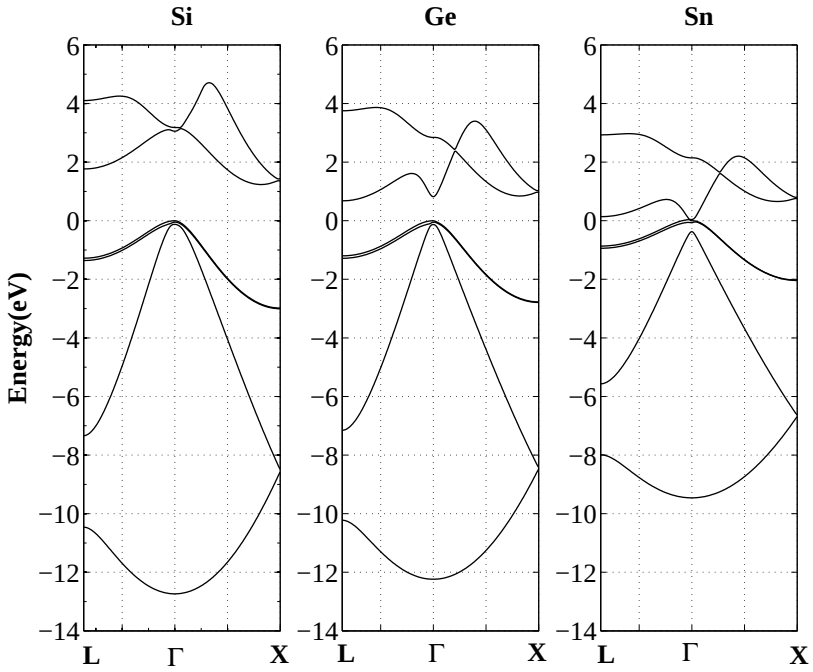

Figure 1. Electronic band structure of Si, Ge, and α-Sn.

3. Alloy models and their validity

Alloy properties can be evaluated either within the virtual crystal approximation (VCA) with identical, average-composition atoms populating the lattice sites of the minimum-volume crystalline unit cell, or by populating individual lattice sites only with pure element atoms, in proportion to the alloy composition ("mixed atom method"), in which case one has to use a supercell, with increased volume. The former is simpler but may be grossly inaccurate in some cases. The latter approach is more realistic, accounting for the effects of disorder and composition fluctuations, but becomes computationally very demanding as the supercell size increases. In this work we used the cubic unit cell with 4 minimum-volume zinc-blende unit cells. This choice enables the binary compositions with 12.5% composition step to be investigated, e.g. the $A_{0.25}B_{0.75}$ alloy is obtained by putting 2 atoms of A and 6 atoms of B in lattice sites. There are different ways for placement of these 8 atoms, each having somewhat different band structure, and the alloy band structure is calculated by averaging over all the possibilities. Within the mixed-atom supercell approach, some care is necessary when "unfolding" the band structure to identify (resolve) the energies at the Γ and X points of the Brillouin zone in the minimum-volume unit cell representation (both are folded onto the supercell Γ point). The lattice constant of an alloy can be estimated from Vegard's law [25]

$$a_0(x)^{AB} = (1-x)a_0^A + xa_0^B, \tag{6}$$

where a_0^A and a_0^B are the lattice constants of elemental crystals of atoms A and B respectively, and a more accurate expression (with bowing) was taken where available.

The first set of test calculations, using both methods, was done for the $Si_{1-x}Ge_x$ alloy. In case of VCA, the pseudopotential was taken to vary linearly between the two constituents [26], i.e.

$$V(q)^{SiGe} = (1-x)V(q)^{Si} + xV(q)^{Ge} \tag{7}$$

where $V(q)^{Si}$ and $V(q)^{Ge}$ are the pseudopotentials of elemental Si and Ge. By the same token, the energy band gap between the top of the valence band at Γ and point g =X, L, or Γ in the conduction band of a binary alloy within the VCA may be expected to be $E_g^{SiGe} = (1-x)E_g^{Si} + xE_g^{Ge}$, but the alloy disorder and other effects make this just the first approximation, and a more accurate dependence is

$$E_g^{SiGe} = (1-x)E_g^{Si} + xE_g^{Ge} + b_{SiGe}x\,(1-x)\,, \tag{8}$$

where b_{SiGe} is a bowing parameter, and the VCA and the mixed-atom method may give quite different values.

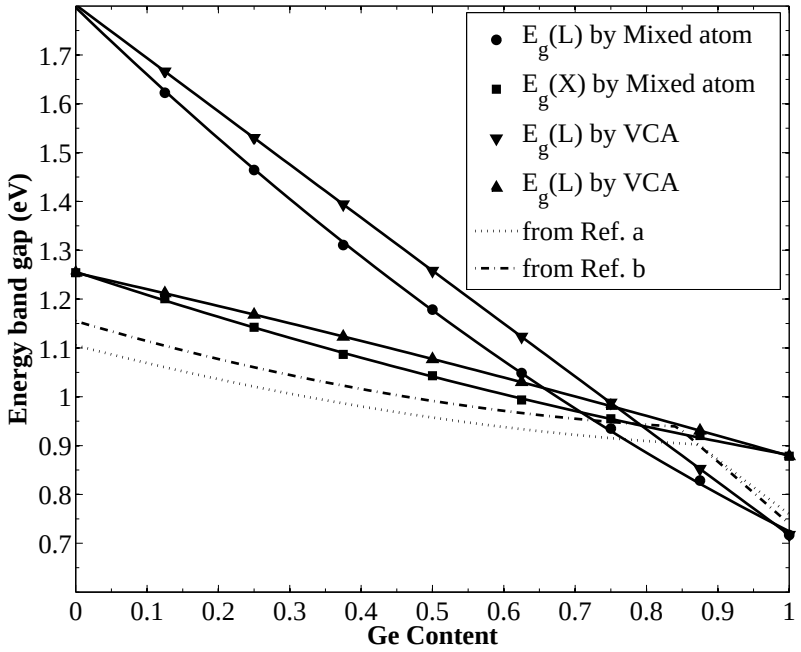

Figure 2. The band gaps of $Si_{1-x}Ge_x$ at X and L points, calculated within the VCA and the mixed-atom method, together with data from the literature (a – Ref. [27], b – Ref. [28]).

The calculated band gaps of $Si_{1-x}Ge_x$ are shown in Fig. 2. We find that the gaps for the X and L valleys, calculated by the mixed atom method, are $E_X = 0.108x^2 + 0.267x + 0.881$ eV and $E_L = 0.335x^2 + 0.738x + 0.724$ eV. Therefore, the bowing parameter of this alloy is 0.33 eV for the Ge content x >0.70 (where the L valley is the lowest), and 0.11 eV for x <0.70 (where the X valley is the lowest). These values are in good agreement with the calculations of S. Krishnamurthy et al. [27], who get the bowing parameters of 0.169 eV and 0.331 eV for the gaps at X and L, and the

experimental value for the gap at X, of 0.206 eV [28] (no bowing of the gap at L point was reported in [28]). On the other hand, the VCA predicts 0.01 eV for $x > 0.75$ and -0.04 eV otherwise.

We have also performed calculations for the (100)-tetragonally distorted (biaxially strained) $Si_{1-x}Ge_x$ alloys, i.e. grown on a relaxed $Si_{1-y}Ge_y$ substrate. The lateral lattice constant $a_{\parallel}(x)$ equals that of the substrate, and in the perpendicular direction it is [29]

$$a_{\perp}(x) = a_0(x)\left(1 - 2\frac{c_{12}(x)}{c_{11}(x)}\frac{a - a_0(x)}{a_0(x)}\right), \tag{9}$$

where c_{11} and c_{12} are the elastic constants [30, 31], given in Table 2 for Si, Ge, and α-Sn, and approximated by Vergard's law for the alloys,

	Si	Ge	Sn
c_{11}(Mbar)	1.67	1.32	0.69
c_{12}(Mbar)	0.65	0.494	0.29

Table 2. Elastic constants c_{11} and c_{12} of Si, Ge, and α-Sn.

$$c(x)^{AB} = (1 - x)c^A + xc^B, \tag{10}$$

where c represents either c_{11} or c_{12}.

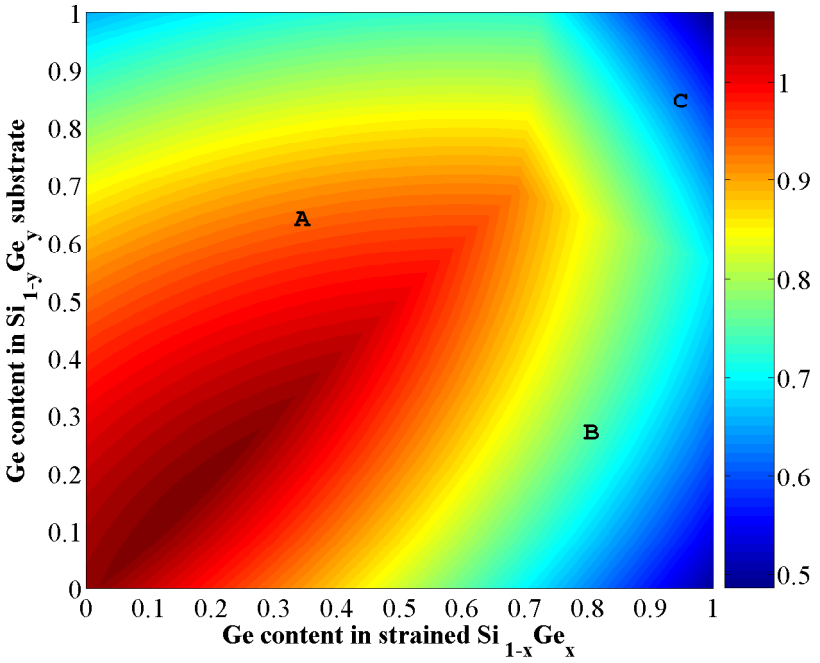

Figure 3. The minimum band gap, in eV, of strained $Si_{1-x}Ge_x$ grown on relaxed $Si_{1-y}Ge_y$.

The results of the calculation for strained $Si_{1-x}Ge_x$ grown on relaxed $Si_{1-y}Ge_y$, Fig. 3, show that the minimum energy gap (of the X valleys parallel to the interface, region B on figures) can be written as $E_{X_{\shortparallel}}(x,y) = 1.069 - 0.425x + 0.533y - 0.152x^2 - 0.324y^2$, and for the perpendicular X valley (region A on figures) as $E_{X_{\perp}}(x,y) = 1.056 + 0.250x - 0.087y - 0.208x^2 - 0.316y^2$, whereas the energy gap for the L valley (region C) is $E_L(x,y) = 1.532 - 0.739x + 0.185y - 0.075x^2 - 0.417y^2$. These results are in good agreement with calculations of Rieger and Vogl [31]: e.g. for strained $Si_{1-x}Ge_x$ grown on Si, with x =0, 0.125, and 0.25 we calculate the band gaps of 1.07, 1.02, and 0.95 eV, respectively, to be compared with 1.07, 1.04, and 1.0 eV [31]. They are also in good agreement with experimental results [32]: 1.17, 1.05, and 0.97 eV. For strained materials it is also worth comparing the deformation potentials. The computational method used in this work, and the conditions (strain along the [001] axis), allow meaningful extraction of:: the uniaxial deformation potential b for the valence band at Γ, the sum of valence and conduction band (at Γ) hydrostatic deformation potentials $a_v + a_c$, and the uniaxial deformation potential Ξ_u^{Δ} of the X (i.e. Δ) valley of the conduction band. We find $a_v + a_c = -6.8$ (-11.5) eV, and $b = -3.75$ (-4.10) eV for Si(Ge), compared to -5.10 (-9.50) eV and -2.10 (-2.90) eV, respectively, for Si(Ge) given in [33]. For Ξ_u^{Δ} we find 11.4 (11.0) eV for Si(Ge), compared to the theoretical values of 9.16 (9.42) eV for Si(Ge) and the experimental value of 8.70 eV for Si, stated in [34]. All these indicate reasonable accuracy of the present method for both strained and unstrained alloys.

4. Results and discussion

In search for direct tunable gap semiconductors, in this section we consider the relaxed $Ge_{1-x}Sn_x$ alloy, strained Ge grown on relaxed $Ge_zSi_xSn_y$ substrate, where $z = 1-x-y$, strained $Ge_{1-x}Sn_x$ grown on relaxed $Ge_{1-y}Sn_y$, and the relaxed $Si_{1-x}Sn_x$ alloy.

4.1. Relaxed $Ge_{1-x}Sn_x$ alloys

In studying of the composition dependence of the band structure of unstrained $Ge_{1-x}Sn_x$ alloy, it is important to note the strong bowing effect in the lattice constant of this alloy, that should be taken into account, even though the size of this effect is not very well known. According to the experimental data for $Ge_{1-x}Sn_x$ from Ref. [35], the lattice constant is given by

$$a_{GeSn}(x) = a_{Sn}x + \theta_{SnGe}x(1-x) + a_{Ge}(1-x), \tag{11}$$

where $\theta_{SnGe} = 0.166$ Å, although its validity has been experimentally established only for the Sn content $\leq$0.2 [35]. Previous calculations [15] have predicted slightly larger value of the bowing parameter, $\approx$0.3 Å, though still in reasonable agreement with the experiment. In our calculations, however, the experimental value was used.

From Fig. 4, which shows the results obtained within the VCA, the Sn content dependence of the band gap for the L valley is $E_L = 0.34x^2 - 0.91x + 0.71$, and for the Γ valley it is $E_\Gamma = 0.78x^2 - 2.00x + 0.87$. The optical (band gap) bowing parameters are

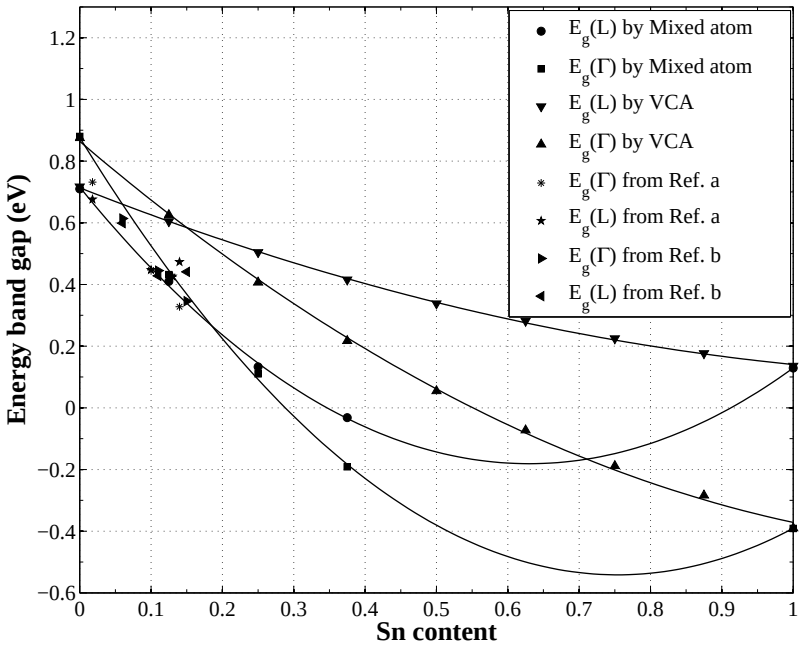

Figure 4. The minimum band gap of relaxed $Ge_{1-x}Sn_x$ for Γ and L valleys, calculated within the VCA and within the mixed atom method. A couple of available experimental values are also displayed (a – Ref. [37], b – Ref. [5]).

clearly much smaller than the above experimental value [1, 5], again showing that the VCA cannot properly predict the composition dependence of the electronic structure of $Ge_{1-x}Sn_x$ alloys. On the other hand, the results presented Fig. 4, obtained within the mixed atom method, show that the relaxed $Ge_{1-x}Sn_x$ alloy has the indirect-to-direct band gap transition at a Sn content of approximately 0.17, with the band gaps for the L and Γ valleys given by $E_L = 2.28x^2 - 2.85x + 0.72$ and $E_\Gamma = 2.49x^2 - 3.76x + 0.88$, respectively. The bowing parameter of relaxed $Ge_{1-x}Sn_x$ alloys is thus 2.49 eV, in good agreement with experiment [5]. The calculated E_Γ in Fig. 4 is also in very good agreement with the measured value (0.41 eV) for $x = 0.14$ from Ref. [1]. For $x = 0.04$, however, their measurement (0.74 eV) shows a somewhat large discrepancy, both in respect to other experiments with similar compositions and to our calculations. The Sn content of 17% for the indirect-to-direct gap transition is also in general agreement with (i.e. in between) the values reported elsewhere, of 15% [36] and 20% [24]. It should also be noted, when comparing theoretical and experimental values for the direct band gap, that the optical measurements of this gap are quite difficult because of small total absorption of actual samples, and measurements necessarily contain a degree of uncertainty.

Finally, it is of interest to compare the calculated and (easier to measure) optical band gap at the L point (E1). For the $Ge_{1-x}Sn_x$ alloy with x =0, 0.125, and 0.25 we find the values of 1.91, 1.414, and 0.99 eV, respectively, and the bowing parameter 2.18

eV, in reasonable agreement with 2.12, 1.83, and 1.60 eV, and the bowing parameter 1.65 eV, reported in [14].

4.2. Strained Ge on relaxed $Ge_{1-x-y}Si_xSn_y$ alloys

This system is currently believed to be of great practical interest, since it offers a direct band gap in Ge at a reasonable level of strain (>1.8%) as well as type-I heterostructure [11] (of importance for realisation of quantum well structures), together with a small thermal expansion mismatch between the two materials [6]. This level of strain is considered acceptable for growth of good quality layers, provided they are below the critical thickness [6] (the same limitation applies to strained $Ge_{1-x}Sn_x$ grown on relaxed $Ge_{1-y}Sn_y$, considered in the next subsection).

In the electronic structure calculations the lattice constant of $Ge_{1-x-y}Si_xSn_y$ alloys was taken to depend on the Si content (x) and Ge content (y) as [35]

$$a_{GeSiSn}(x,y) = a_{Ge} + \triangle_{SiGe}x + \theta_{SiGe}(1-x) + \triangle_{SnGe}y + \theta_{SnGe}y(1-y), \quad (12)$$

where $\triangle_{SiGe} = a_{Si} - a_{Ge}$, $\triangle_{SnGe} = a_{Sn} - a_{Ge}$, and $\theta_{SiGe} = -0.026$ Å.

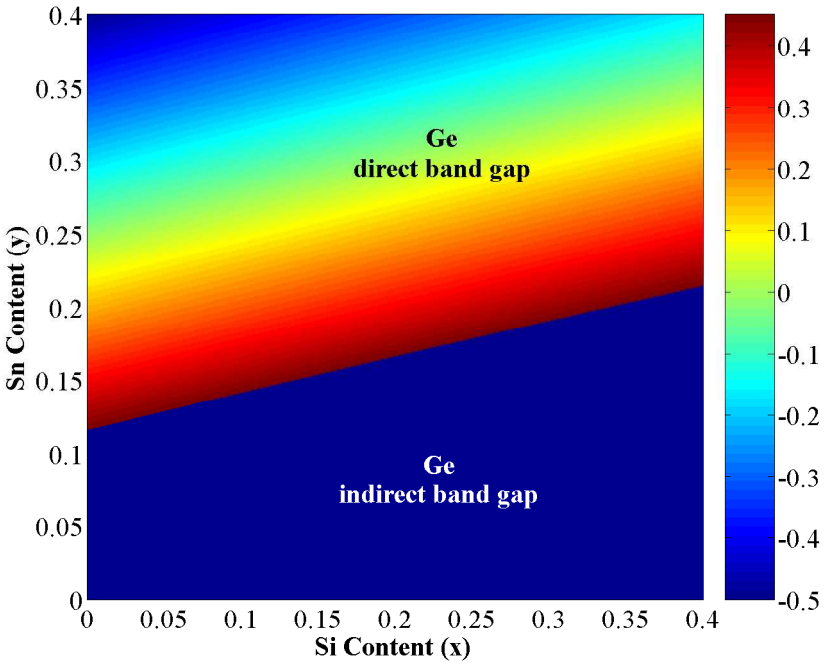

Figure 5. Band gap energy (in eV) of strained Ge grown on relaxed $Ge_{1-x-y}Si_xSn_y$ alloys.

The band gap for the L valley is was now found to be described as $E_L(x,y) = 0.723 + 0.564x - 2.352y + 0.189xy - 0.074x^2 + 0.068y^2$, while the band gap for Γ valley is $E_\Gamma(x,y) = 0.880 + 0.929x - 3.807y - 0.160xy - 0.078x^2 + 0.937y^2$, where x and y denote the content of Si and Sn, respectively. The line defined by $E_L = E_\Gamma$ in the x-y plane is

the boundary between regions where the band gap of strained Ge is direct or indirect. A direct band gap is achieved for sufficiently large tensile strain of Ge, achievable by growing it on appropriate $Ge_{1-x-y}Si_xSn_y$ alloy substrate, as given in Fig. 5.

4.3. Strained $Ge_{1-x}Sn_x$ on relaxed $Ge_{1-y}Sn_y$ alloys

For this calculation one needs the elastic constants for the GeSn alloy. This was estimated by linear interpolation, since no quadratic correction parameter for this alloy is known. The band gap for the L valley is now found to be described by $E_L(x,y) = 0.672 - 1.794x - 1.181y + 8.780xy - 2.958x^2 - 3.925y^2$, and for the Γ valley by $E_\Gamma(x,y) = 0.782 - 1.483x - 2.577y + 8.216xy - 1.653x^2 - 1.866y^2$, where x and y denote the Sn content in strained $Ge_{1-x}Sn_x$ layer and in relaxed $Ge_{1-y}Sn_y$ substrate, respectively. Here again we find the region in the parameter space that corresponds to a direct band gap semiconductor, achieved by the combined influence of material composition and tensile strain, Fig. 6.

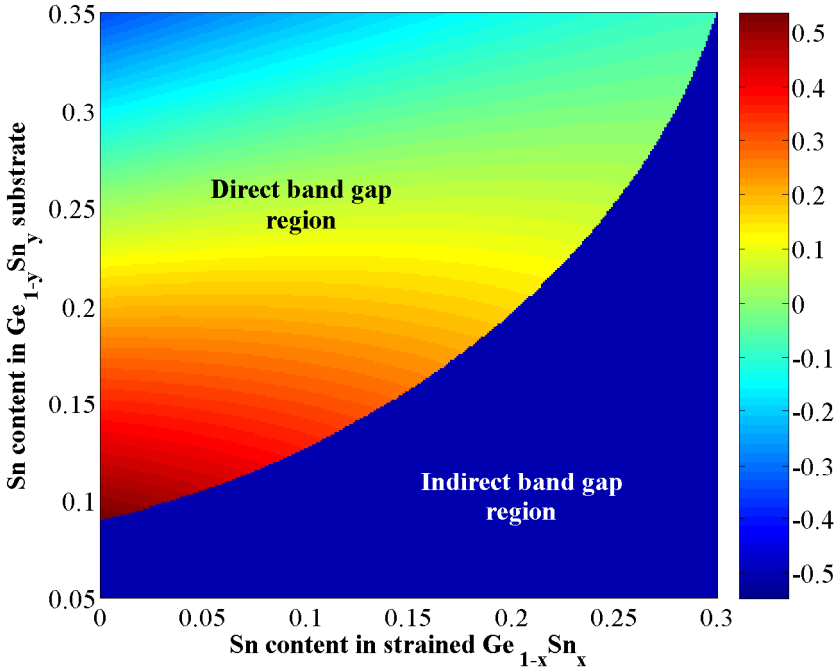

Figure 6. The minimum band gap (in eV) of strained $Ge_{1-x}Sn_x$ grown on relaxed $Ge_{1-y}Sn_y$ alloys.

4.4. Relaxed $Si_{1-x}Sn_x$ alloys

In this calculation the lattice bowing parameter of the alloy lattice constants of SiSn alloys was set to zero. Its value has not been experimentally determined, and (although it may seem a bit surprising in view of a very large difference in atomic radii) the very

recent LDA calculations [38] predict a negligible deviation of SiSn alloy lattice constant from the Vegard's law.

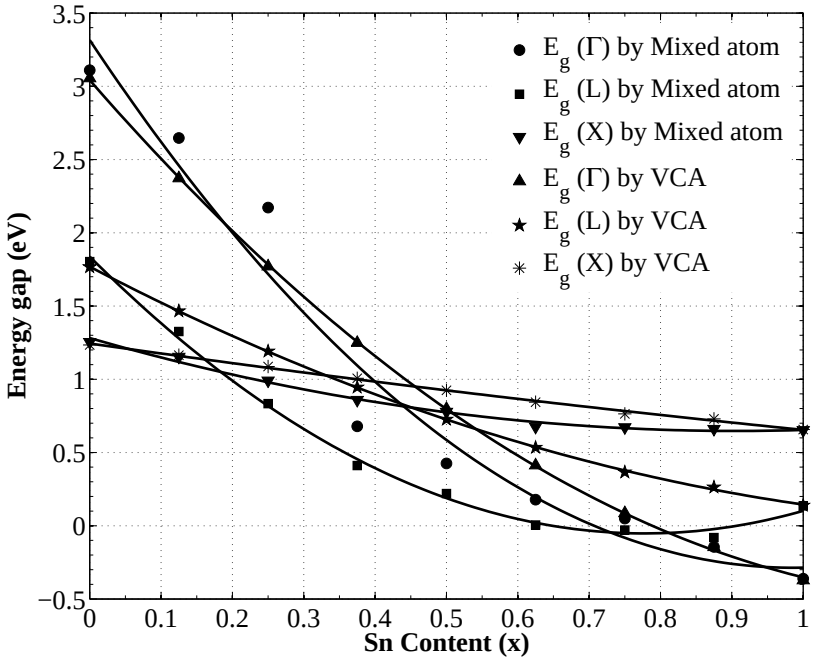

Figure 7. The minimum energy band gap (in eV) of relaxed $Si_{1-x}Sn_x$ alloy, calculated within the VCA and within the mixed atom method.

Within the mixed atom method, the band gaps for the L and X valleys in relaxed $Si_{1-x}Sn_x$ alloy were found to be given by $E_L(x) = 1.837 - 4.860x + 3.124x^2$ and $E_X(x) = 1.281 - 1.399x + 0.772x^2$, respectively, while the band gap for the Γ valley is $E_\Gamma(x) = 3.315 - 7.316x + 3.715x^2$, where x is the Sn content (Fig. 7). On the other hand, the VCA calculation gives the band gaps for L, X and Γ valleys as $E_L(x) = 1.768 - 2.549x + 0.925x^2$, $E_X(x) = 1.244 - 0.691x + 0.100x^2$, and $E_\Gamma(x) = 3.042 - 5.588x + 2.193x^2$, respectively. Therefore, the VCA predicts the indirect-to-direct band gap transition in the relaxed $Si_{1-x}Sn_x$ when the Sn content exceeds approximately 0.55, while the (more accurate) mixed atom method does not show any such transition. This finding may be contrasted to the indication given in the recent work [38] that the direct-indirect crossover in SiSn occurs at approx 25% Sn. This was reached using the LDA and (in contrast to our calculation) accounting for the atomic position relaxation, but in order to overcome the well-known LDA shortcomming in the bandgap prediction the "scissors" correction was employed, which itself brings in a degree of uncertainty. It is therefore fair to conclude that the question of the direct band gap in SiSn alloy is still open.

5. Conclusion

Using local density functional theory and the self-consistent pseudo-potential plane wave method we have explored some important properties of GeSiSn alloys, relevant for optoelectronic applications. In particular, we have studied relaxed $Ge_{1-x}Sn_x$ alloys, strained Ge grown on relaxed $Ge_{1-x-y}Si_xSn_y$ alloys, strained $Ge_{1-x}Sn_x$ grown on relaxed $Ge_{1-y}Sn_y$ alloys and relaxed Sn_xSi_{1-x} alloys. These were modelled by the mixed atom method, the accuracy of which proved to be far better than that of the virtual crystal approximation, using the available experimental data for comparison. Band structure calculations show that relaxed $Ge_{1-x}Sn_x$ alloys have an indirect-to-direct band gap cross-over at a Sn content of $\approx$0.17, with the bowing parameter equal to 2.49 eV. Furthermore, calculations for strained Ge on relaxed $Ge_{1-x-y}Si_xSn_y$ ternary alloys, and for strained $Ge_{1-x}Sn_x$ grown on relaxed $Ge_{1-y}Sn_y$ alloys, give the range of the substrate compositions and Sn content which lead to direct band gap materials. In contrast, within the mixed-atom approach the Sn_xSi_{1-x} alloys never show a finite direct band gap (while the VCA calculation does predict it).

References

[1] M. R. Bauer, J, Tolle, C. Bungay, A. V. G. Chizmeshya, D. J. Smith, J. Menéndez, and J. Kouvetakis, Solid State Communications **127**, 355 (2003).
[2] R. Ragan, K. S. Min, and H. A. Atwater, Materials Science and Engineering B **87**, 204 (2001).
[3] W. Wegscheider, K. Eberl, U. Menczigar, and G. Abstreiter, Appl. Phys. Lett. **57**, 204 (1990).
[4] O. Gurdal, M. A. Hasan, M. R. Sardela, Jr., J. E. Greene, J. E. Greene, H. H. Radamson, J. E. Sundgren, and G. V. Hansson, Appl. Phys. Lett. **67**, 956 (1995).
[5] G. He, and H. A. Atwater, Phys. Rev. Lett. **79**, 1937 (1997).
[6] J. Kouvetakis, J. Menéndez, and A. G. V. Chizmeshya, Annual Review of Materials Research **36**, 497 (2006).
[7] J. Tolle, R. Roucka, A. G. V. Chizmeshya, J. Kouvetakis, V. R. D'Costa, and J. Menéndez, Appl. Phys. Lett. **88**, 252112 (2006).
[8] C. S. Cook, S. Zollner, M. R. Bauer, P. Aella, J. Menéndez, and J. Kouvetakis, Thin Solid Films **455-456**, 217 (2004).
[9] R. A. Soref, and C. H. Perry, J. Appl. Phys. **69**, 593 (1991).
[10] R. Soref, and L. Friedman, Superlattices and Microstructures **14**, 189 (1993).
[11] J. Menéndez, and J. Kouvetakis, Appl. Phys. Lett. **85**, 1175 (2004).
[12] D. W. Jenkins, and J. D. Dow, Phys. Rev. B **36**, 7994 (1987).
[13] K. A. Mäder, A. Baldereschi, and M. von Kanel, Solid State Commum. **69**, 1123 (1989).
[14] V. R. D'Costa, C. S. Cook, A. G. Birdwell, C. L. Littler, M. Canonico, S. Zollner, J. Kouvetakis, and J. Menéndez, Phys. Rev. B **73**, 125207 (2006).
[15] Y. Chibane, B. Bouhafs, and M. Ferhat, Phys. Stat. Sol. (b) **240**, 116 (2003).
[16] J. E. Bernard, and A. Zunger, Phys. Rev. B **36**, 3199 (1987).
[17] W. Kohn, and L. J. Sham, Phys. Rev. **140**, A1133 (1965).
[18] R. M. Martin, *Electronic Structure; Basic Theory and Practical Methods* (Cambridge University Press, Cambridge, 2004).
[19] J. C. Slater, *Self-consistent Field for Molecules and Solids* (McGraw-Hill, New York, 1974).
[20] M. Schluter, J. R. Chelikowsky, S. G. Louie, and M. L. Cohen, Phys. Rev. **12**, 4200 (1975).
[21] G. P. Srivastava, J. Phys. C **15**, 707 (1982).

[22] E. Kaxiras, *Atomic and Electronic Structure of Solids* (Cambridge University Press, Cambridge, 2003).
[23] P. E. Blochl, O. Jepsen, and O. K. Andersen, Phys. Rev. B **49**, 16223 (1994).
[24] J. D. Sau, and M. L. Cohen, Phys. Rev. B **75**, 045208 (2007).
[25] L. Vegard, Z. Phys. **5**, 17 (1921).
[26] P. Harrison, *Quantum Wells, Wires and Dots; Theoritical and Computational Physics* (John Wiley Sons, Chichester, 2005).
[27] S. Krishnamurthy, S. Sher, and A. Chen, Appl. Phys. Lett. **47**, 160 (1985).
[28] J. Weber, and M. I. Alonso, Phys. Rev. B **40**, 5683 (1989).
[29] S. C. Jain, J. R. Willis, and R. Bullough, Adv. Phys. **39**, 127 (1990).
[30] N. Bouarissa, and F. Annane, Materials Science and Engineering B **95**, 100 (2002).
[31] M. M. Rieger, and P. Vogl, Phys. Rev. B **48**, 14276 (1993).
[32] D. Dutatre, G. Bremond, A. Souifi, and T. Benyattou, Phys. Rev. B **44**, 11525 (1991).
[33] S. Ridene, K. Boujdoria, H. Bouchriha, and G. Fishman, Phys. Rev. B **64**, 085329 (2001).
[34] C. van de Walle, Phys. Rev. B **39**, 1871 (1989).
[35] P. Aella, C. Cook, J. Tolle, S. Zollner, A. V. G. Chizmeshya, and J. Kouvetakis, Appl. Phys. Lett. **84**, 888 (2004).
[36] M. Bauer, J. Taraci, J. Tolle, A. V. G. Chizmeshya, S. Zollner, D. J. Smith, J. Menendez, C. Hu, and J. Kouvetakis, Appl. Phys. Lett. **81**, 2992 (2002).
[37] H. P. L. de Guevara, A. G. Rodríguez, H. Navarro-Contreras, and M. A. Vidal, Appl. Phys. Lett. **84**, 4532 (2004).
[38] J. Tolle, A. V. G. Chizmeshya, Y. Y. Fang, J. Kouvetakis, V. R. D'Costa, C. W. Hu, J. Menendez, and I. S. T. Tsong, Appl. Phys. Lett. **89**, 231924 (2006).